



Fiber–Wireless Integrated Reliable Access Network for Mobile Fronthaul Using Synclastic Uniform Circular Array with Dual–Mode OAM Multiplexing

Abstract: We propose an access network that integrates fiber and wireless for mobile fronthaul (MFH) with simple protection capabilities, using dual-mode orbital angular momentum (OAM) multiplexing. We experimentally demonstrate a 3.35 Gbit/s DMT-32QAM pre-equalized system with 10 km and 15 km fiber links in the 5.9 GHz band; then there is a link of two channels with a 0.5 m wireless link.

Keywords: OAM; fiber-wireless integrated access network

XU Yusi, WU Xingbang, YANG Guomin, and CHI Nan

(Fudan University, Shanghai 430074, China)

DOI: 10.12142/ZTECOM.201904010

<http://kns.cnki.net/kcms/detail/34.1294.tn.20191209.1328.009.html>, published online December 9, 2019

Manuscript received: 2019-01-31

1 Introduction

Driven by emerging mobile devices and mobile multimedia, mobile data traffic is exponentially increasing. Different multiplexing technologies are researched and discussed. In order to provide end users with multi-gigabit wireless link rates, fiber-wireless integrated access networks have proven their potential for more efficient traffic offload and flexibility [1] – [5]. Millimeter wave (MMW) that provides a friendly infrastructure for high-throughput wireless services with low cost, abundant bandwidth, and rapid deployment is an efficient physical link for mobile fronthaul (MFH), which has been extensively studied. Photonics-aided MMW generation for the MFH that can leverage existing fiber to the home (FTTH), passive optical network (PON), and wavelength division multiplexing (WDM) PON in the future [2] – [6]. However, tree-based network topologies lack simple and cost-effective protection or recovery capabilities.

At the same time, orbital angular momentum (OAM) has been proposed as an emerging multiplexing technique to further improve spectral efficiency and channel capacity in radio communications due to mutual orthogonality of different modes [7] – [9]. In principle, many orthogonal modes of OAM can be used

for multiplexing and demultiplexing with low crosstalk. Therefore, using various antennas to generate OAM beams in the radio domain has been extensively studied in the research community. By simultaneously transmitting different OAM modes, synclastic uniform circular array (UCA) has attracted increasing interest. Based on the multi-layer design, a synclastic UCA is proposed for OAM generation and dual mode communication [8] – [10]. The integration of OAM in the low-frequency radio domain and optical fiber for MFH is an attractive alternative.

In this paper, we propose a fiber-wireless reliable access network for MFH, which integrates fiber and wireless with dual-mode OAM multiplexing to verify the performance of an optical OAM transmission architecture based on DMT technology. Two modes from one synclastic UCA are assigned two different fiber links that may have simple protection capabilities. We experimentally demonstrate a 3.35 Gbit/s DMT-32QAM fiber-wireless integrated system with pre-equalization (Pre-EQ) in the 5.9 GHz band. After 10 km and 15 km fiber transmission, the two modes are transmitted simultaneously through a 0.5 m wireless link respectively.

2 Principle of Antenna

The synclastic UCA, in which the elements are placed in a circular ring and have the same orientation, is an array configuration of very practical interest. A typical synclastic UCA mod-

This work is supported by ZTE Industry–Academia–Research Cooperation Funds under Grant No. 2016ZTE04–01.

el with eight elements is presented in **Fig. 1** and the corresponding free space propagation geometry with synclastic UCAs is also illustrated. In **Fig. 1b**, we assume that N isotropic elements are equally placed on the $x - y$ plane along a circular ring with radius of a . The normalized field of the whole array can be written as

$$\begin{aligned} E_n &= \sum_{n=1}^N a_n \cdot /R_n \\ a_n &= I_n e^{j\varphi_n} = I_n e^{j(\varphi_0 + n \cdot 2\pi l/N)} \\ E_{nn'} &= \frac{e^{-jkr}}{r} \sum_{n=1}^N a_n I_n e^{j[k\sin\theta\cos(\phi_{n'} - \phi_n) + \varphi_{n'} + \varphi_n]}, \end{aligned} \quad (1)$$

where k is the Boltzmann constant, R_n is the distance from the n th array element to the n' -th observation element, and a_n is the

$$a_n = I_n e^{j\varphi_n} = I_n e^{j(\varphi_0 + n \cdot 2\pi l/N)}, \quad (2)$$

where I_n is the amplitude excitation and φ_n is the phase excitation of the n -th element. And φ_0 is the assumed system reference phase, N is the number of the elements of an array, and l is the mode of the OAM.

Assuming that $r \gg a$ and $R_n \approx r$, the electric field of the n' -th element in the receiving array transmitted by the n -th element in the transmitting array is

$$E_{nn'} = \frac{e^{-jkr}}{r} \sum_{n=1}^N a_n I_n e^{j[k\sin\theta\cos(\phi_{n'} - \phi_n) + \varphi_{n'} + \varphi_n]}, \quad (3)$$

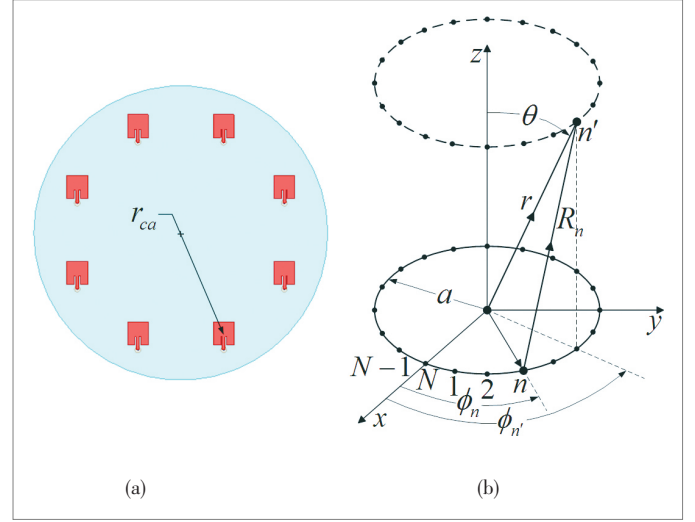
where $\varphi_{n'}$ is the phase of the element in the receiving array. Thus, the electric field of the n' -th element in the receiving array can be derived as

$$\begin{aligned} E_{n'} &= \frac{e^{-jkr}}{r} \sum_{n=1}^N a_n I_n e^{j[k\sin\theta\cos(\phi_{n'} - \phi_n) + \varphi_{n'} + \varphi_n]} = \\ & \left[\frac{e^{-jkr}}{r} \sum_{n=1}^N I_n e^{j[k\sin\theta\cos(\phi_{n'} - \phi_n) + 2\varphi_0 + n \cdot 2\pi l/N]} \right] \cdot e^{jn' \cdot 2\pi l/N}. \end{aligned} \quad (4)$$

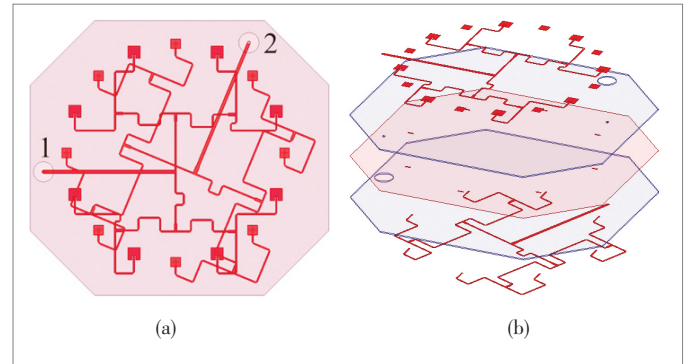
Finally, the phase factor of $e^{jn' \cdot 2\pi l/N}$ is extracted from Equation (4), which proves the OAM generation from these equal phase and equal amplitude UCAs theoretically.

To verify the correctness of the theory, a dual-mode OAM multiplexing antenna is designed and fabricated (**Fig. 2**). And the near field phase front of the OAM antenna is simulated and the result is shown in **Fig. 3**, which indicates the reliable generation of the OAM beams.

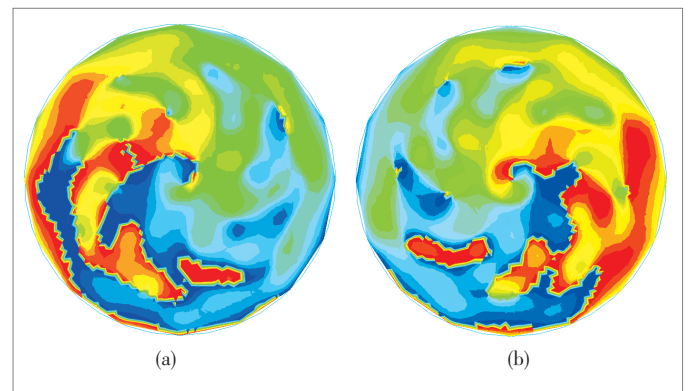
While OAM has unlimited range of achievable states which are mutually orthogonal, it is quite promising to combine it with optical fiber for MFH to achieve high spectrum efficiency transmission. The wireless OAM multiplexing is achieved by the synclastic UCAs with N independent OAM modes. The



▲ **Figure 1.** Synclastic UCA model: (a) Top view; (b) schematic diagram (the upper array is the receiving array and the lower array is the transmitting array).



▲ **Figure 2.** Dual-mode OAM antenna: (a) Top view; (b) explosive view.



▲ **Figure 3.** Near field phase front of the dual mode OAM antenna: (a) +1 mode; (b) +2 modes.

various OAM beams can be considered as a form of spatial division multiplexing (SDM). The OAM beams multiplexed with different modes propagate along the same spatial axis in free space. The coaxially propagating OAM beams lead to inherently low crosstalk between OAM channels and reduce the need for signal processing to eliminate OAM channel interference af-

ter demultiplexing.

As we can see, OAM provides another degree of freedom to carry information with multi-level amplitude/phase modulation. It shows potential possibility to integrate OAM with the current fiber-based MFH infrastructure for further increase of system capacity.

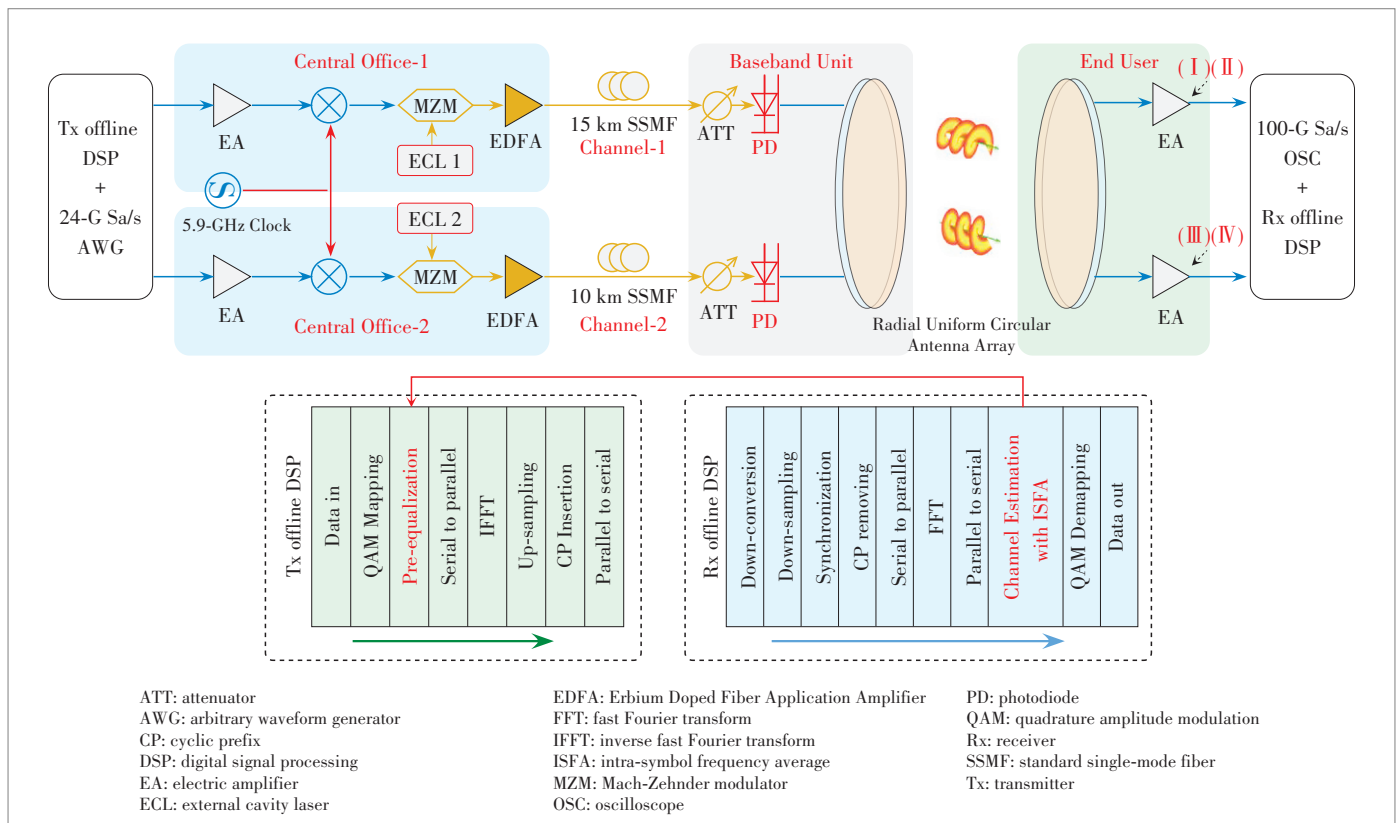
3 Experimental Setup

An experimental setup for intensity modulation and direct detection (IM-DD) DMT-32QAM signal transmission based on the Mach-Zehnder modulator (MZM) is shown in Fig. 4. The DMT signal is generated offline in Matlab in a 32-QAM modulation format. We estimate the channel using 256 subcarriers loaded with data and 10 training sequences. We use 1/32 subcarriers as the cyclic prefix (CP) to avoid inter-symbol interference (ISI) as well. For Rx offline digital signal processing (DSP), data without Pre-EQ are first sent for channel estimation with intra-symbol frequency domain averaging (ISFA), and then Pre-EQ is operated using the estimated reverse channel [11].

The experimental system consists of two independent central offices (COs) with MZM modulators that convert the signal to optical domain. The baseband unit (BBU) is used for dual-mode OAM beams transmission and the end user side is used to receive signals. Two COs are connected to both sides of a synclastic UCA array using the 15-km and 10-km SSMF links

as Ch-1 and Ch-2 respectively. These different fiber links may have simple protection features. The 200 Mbit/s baseband DMT-32QAM signal is uploaded into an arbitrary waveform generator (AWG) with 1.2 - 2.4 GSa/s sample rate for Ch-1 and Ch-2. The amplified signal is then mixed with a 5.9 GHz clock and up-converted into two intermediate frequency (IF) signals. The modulated signal through the MZM is then amplified by the Erbium Doped Fiber Application Amplifier (EDFA) prior to fiber transmission. After transmission, an optical attenuator (ATT) is applied to adjust the received optical power maintained at 0 dBm before power is injected into the photodiode (PD). Then, the converted electrical signals are injected into the synclastic UCA and performed in two orthogonal OAM modes respectively. After 50-cm free space transmission, radio beams with different OAM modes are detected by the according received antenna. Finally, the received signals are amplified and sent into an oscilloscope (OSC) at a 12.5 GSa/s sample rate, which is then processed by the Rx offline DSP.

In another experiment, the arbitrary waveform generator (AWG, Tektronix 7122C) is used to generate a 1.6 GSa/s DMT signal with a carrier frequency of 5.9 GHz. A 1550 nm external cavity laser (ECL) is used as an optical carrier and fed into the intensity modulator. The signal is converted into optical domain via a MZM. The optical power is controlled by a variable optical attenuator (VOA) before transmitting the signal through standard single mode fiber (SSMF). At the receiver

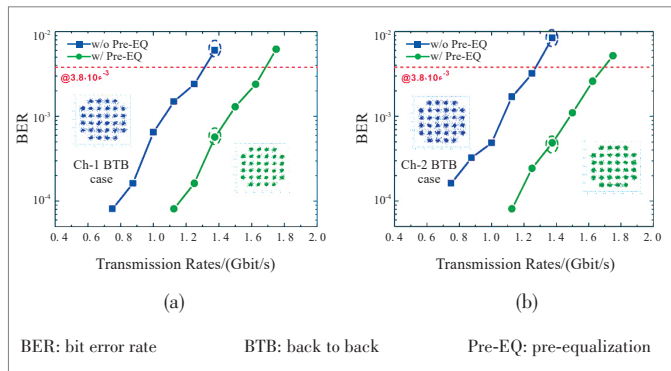


▲ Figure 4. Experimental setup for intensity modulation and direct detection (IM-DD) DMT-32QAM signal transmission based on the MZM.

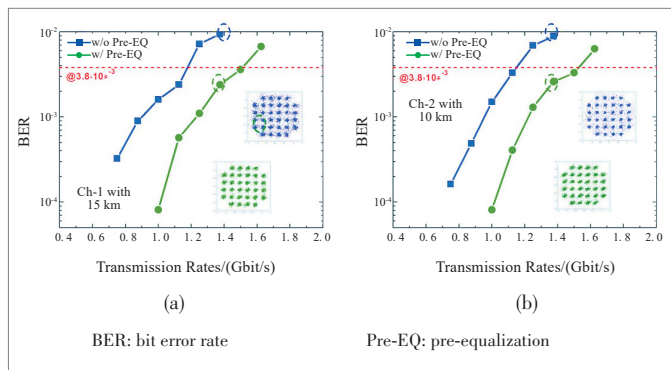
side, the optical signal is detected by a PD to achieve photoelectric conversion. The electrical signal is amplified before being transmitted to the synclastic UCA. After 40 cm free space transmission, the electrical signal is received by the antenna of the receiver. The received signal is then sampled using a 12.5 GSa/s digital storage oscilloscope (DSO Tektronix DSA73304D) and the off-line DSP is processed.

4 Results and Analysis

For the first experiment, Figs. 5a and 5b show the bit error rate (BER) of Ch-1 and Ch-2 versus transmission rates in the case of back to back (BTB). The blue lines indicate the signal without Pre-EQ and the green lines represent the signal with Pre-EQ. We observe that the BER performance of Ch-1 and Ch-2 at the same transmission rate is similar with or without Pre-EQ. As can be seen from Figs. 5a and 5b, the BER increases as the rate increases. A DMT-32QAM signal exceeding 1.125 Gbit/s can be delivered below the BER of 3.8×10^{-3} per channel without Pre-EQ. In addition, the use of Pre-EQ can effectively increase the transmission rate to over 1.625 Gbit/s. In the case of BTB with Pre-EQ, both the channels can realize a total rate of 3.35 Gbit/s. Figs. 6a and 6b show the BER of Ch-1

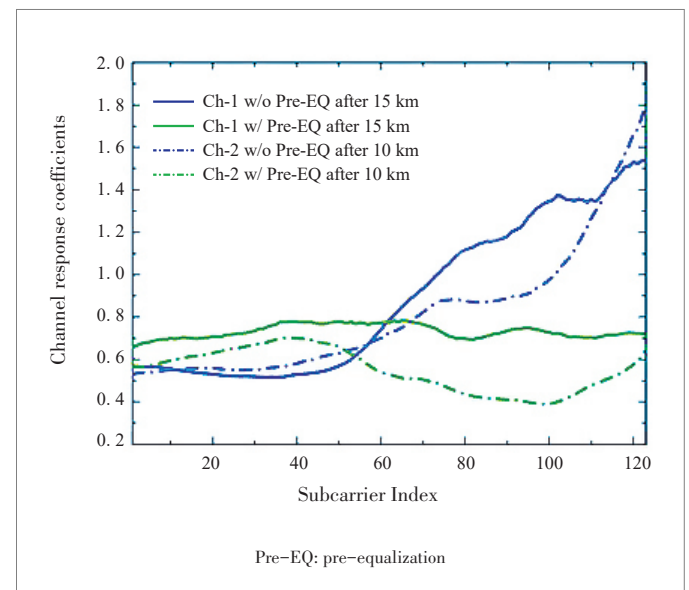


▲ Figure 5. (a) The BER of Ch-1 vs. transmission bit rates under BTB case without and with Pre-EQ; (b) the BER of Ch-2 vs. transmission bit rates under BTB case without and with Pre-EQ.

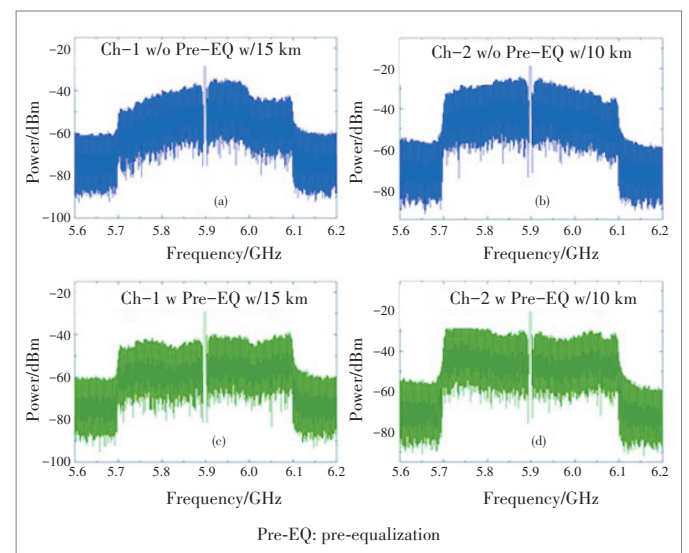


▲ Figure 6. (a) The BER of Ch-1 vs. transmission bit rates after 15 km fiber without and with Pre-EQ; (b) the BER of Ch-2 vs. transmission bit rates after 10 km fiber without and with Pre-EQ.

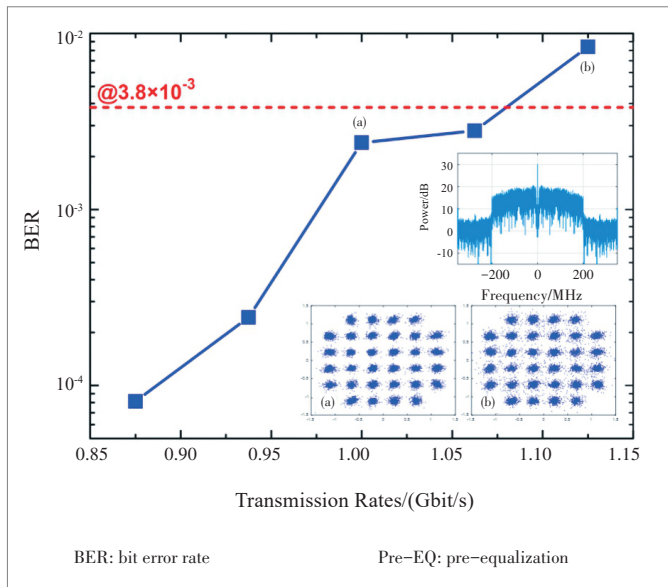
and Ch-2 versus the transmission rate after 15 km and 10 km fiber transmission respectively. With Pre-EQ, the transmission rate of both channels can be effectively increased from 1.125 Gbit/s to 1.5 Gbit/s. For dual-mode OAM multiplexing, a total 3 Gbit/s rate can be achieved. Constellations of DMT-32QAM signal at 1.375 Gbit/s without or with Pre-EQ are shown in the insets with blue and green markers respectively. The channel responses of Ch-1 and Ch-2 are shown in Fig. 7, which shows that the channel response coefficients can be flattened with Pre-EQ. As can be seen from Fig. 8, the channel response coefficients after 15 km transmission exceed the channel response coefficients after 18 km transmission with subcarrier index increasing.



▲ Figure 7. The channel response coefficients of Ch-1 and Ch-2 without and with Pre-EQ.



▲ Figure 8. The electrical spectra of the received DMT-32QAM signal without and with Pre-EQ.



▲ Figure 9. BER versus transmission bit rates for integrated fiber and OAM wireless transmission links.

Figs. 8a - d are the spectra of the received DMT-32QAM signals with and without Pre-EQ respectively. It indicates that the spectrum can be flush with the Pre-EQ as well. In this experiment, Ch-1 and Ch-2 were simultaneously transmitted. However, if one of the fiber links fails, the other link will not be affected. Therefore, data switching protection can be implemented based on service priority.

For the second experiment, the BER vs. transmission rates (Fig. 9) indicates that the signal transmission of 1.0625 Gbit/s can reach the 7% Forward error correction (FEC) threshold ($BER = 3.8 \times 10^{-3}$), which is even worse if the transmission rate is increased. The electrical spectrum of the down-converted 200 Mbaud DMT-32QAM signal and the constellations of 1 Gbit/s and 1.125 Gbit/s are shown in the insets respectively.

5 Conclusions

In this paper, a fiber-wireless reliable access network for MFH is proposed through the integration of fiber and wireless with dual-mode OAM multiplexing. We experimentally demonstrated a 3 Gbit/s DMT-32QAM fiber-optic wireless integrated system with a synclastic UCA. The system has Pre-EQ in the 5.9 GHz band, and both channels after 10 km and 15 km fiber transmission are transmitted over a 0.5-m wireless link simultaneously. The fiber-wireless reliable access network can alternatively be used for MFH.

References

[1] CHANG G K, CHENG L, XU M, et al. Integrated Fiber-Wireless Access Architecture for Mobile Backhaul and Fronthaul in 5G Wireless Data Networks [C]// IEEE Avionics, Fiber-Optics and Photonics Technology Conference (AVFOP), Atlanta, USA, 2014. DOI:10.1109/avfop.2014.6999461

[2] YU J J, HUANG M F, JIA Z S, et al. Polarization-Insensitive All-Optical Upconversion for Seamless Integration Optical Core/Metro/Access Networks with ROF Systems Based on a Dual-Pump FWM Scheme [J]. Journal of Lightwave Technology, 2009, 27(14): 2605 - 2611. DOI:10.1109/jlt.2009.2013364

[3] YU J J, CHANG G-K, JIA Z S, et al. Cost-Effective Optical Millimeter Technologies and Field Demonstrations for very High Throughput Wireless-Over-Fiber Access Systems [J]. Journal of Lightwave Technology, 2010, 28(16): 2376 - 2397. DOI:10.1109/jlt.2010.2041748

[4] ZHANG J W, WANG J, XU Y M, et al. Fiber-Wireless Integrated Mobile Backhaul Network Based on a Hybrid Millimeter-Wave and Free-Space-Optics Architecture with an Adaptive Diversity Combining Technique [J]. Optics Letters, 2016, 41(9): 1909 - 1912. DOI:10.1364/ol.41.001909

[5] CHENG L, ZHU M, MUHAMMAD U G, et al. Adaptive Photonics-Aided Coordinated Multipoint Transmissions for Next-Generation Mobile Fronthaul [J]. Journal of Lightwave Technology, 2014, 32(10): 1907 - 1914

[6] GOU P Q, KONG M, YANG G M, et al. Integration of OAM and WDM in Optical Wireless System by Radial Uniform Circular Array [J]. Optics Communications, 2018, 424: 159 - 162. DOI:10.1016/j.optcom.2018.04.059

[7] FANG Y, YU J J, ZHANG J W, et al. Ultrahigh-capacity Access Network Architecture for Mobile Data Backhaul Using Integrated W-band Wireless and Free-space Optical Links with OAM Multiplexing [J]. Optics Letters, 2014, 39(14): 4168 - 4171. DOI:10.1364/ol.39.004168

[8] BAI Q, TENNANT A, ALLEN B. Experimental Circular Phased Array for Generating OAM Radio Beams [J]. Electronics Letters, 2014, 50(20): 1414 - 1415. DOI:10.1049/el.2014.2860

[9] YAO A M, PADGETT M J. Orbital Angular Momentum: Origins, Behavior and Applications [J]. Advances in Optics and Photonics, 2011, 3(2): 161 - 204. DOI: 10.1364/aop.3.000161

[10] LI F, YU J J, FANG Y, et al. Demonstration of DFT-Spread 256QAM-OFDM Signal Transmission with Cost-effective Directly Modulated Laser [J]. Optics Express, 2014, 22(7): 8742 - 8748. DOI:10.1364/oe.22.008742

Biographies

XU Yusi is with the Key Laboratory for Information Science of Electromagnetic Waves, Department of Communication Science and Engineering, School of Information Science and Technology, Fudan University, China.

WU Xingbang (18210720075@fudan.edu.cn) is with Department of Communication Science and Engineering, School of Information Science and Technology, Fudan University, China. She received the B. S. degree in electronic science and technology (electronic materials and components) from South China University of Technology, China in 2017. She is currently a master degree candidate at Fudan University and engaged in visible light communications.

YANG Guomin is with the Key Laboratory for Information Science of Electromagnetic Waves, Department of Communication Science and Engineering, School of Information Science and Technology, Fudan University, China.

CHI Nan is with Department of Communication Science and Engineering, School of Information Science and Technology, Fudan University, China. She received the B. S. and Ph. D. degrees in electrical engineering from Beijing University of Posts and Telecommunications, China in 1996 and 2001, respectively. From July 2001 to December 2004, she worked as assistant professor at the Research Center COM, Technical University of Denmark. From January 2005 to April 2006, she was a research associate at the University of Bristol, United Kingdom. She has received the New Century Excellent Talents Awards from the Education Ministry of China, Shanghai Shu Guang scholarship, Japanese OKAWA intelligence Fund Award, Pujiang talent of Shanghai City, and Ten Outstanding IT Young Persons Awards of Shanghai City. Her research interests are in the area of coherent optical transmission, visible light communication, and optical packet/burst switching.